Ordered Structures in Polycarbonate Studied by Infrared and Raman Spectroscopy, Wide-Angle X-ray Scattering, and Differential Scanning Calorimetry

J. Dybal,* P. Schmidt, J. Baldrian, and J. Kratochvíl

Institute of Macromolecular Chemistry, Academy of Sciences of the Czech Republic, 162 06 Prague 6, Czech Republic

Received May 12, 1998; Revised Manuscript Received July 13, 1998

ABSTRACT: Ordered structures in samples of Bisphenol A polycarbonate (BPAPC) prepared by varying thermal and solvent conditions were investigated by infrared and Raman spectroscopy, wide-angle X-ray scattering (WAXS), and differential scanning calorimetry (DSC). Based on the spectroscopic analysis and ab initio quantum mechanical calculations of diphenyl carbonate as a model compound, an assignment of the bands conformationally sensitive to the *trans*−*trans* and *cis*−*trans* structures is proposed. Temperature dependences of the vibrational spectra of BPAPC show that *cis*−*trans* structure is the energetically preferred conformation in the amorphous state and in solution and its population can be increased with decreasing temperature in amorphous BPAPC even below the glass transition temperature. Differences in the degrees of ordering in semicrystalline BPAPC assessed from the vibrational spectra, WAXS, and DSC indicate partial order in the interfacial region between the crystalline and amorphous phases. In some solvents (toluene, benzene), aggregation of BPAPC occurs, leading to the ordered structure analogous to crystalline BPAPC. The order is preserved in semicrystalline BPAPC obtained by the room-temperature evaporation of the solvent.

Introduction

Conformational structure and intermolecular arrangement in glassy and semicrystalline polycarbonate of 4,4′-isopropylidenediphenol (Bisphenol A polycarbonate (BPAPC)) (structure I) and its relation to the bulk mechanical

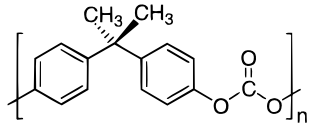

I

properties have received much attention. A number of investigations have been done using both experimental and theoretical methods to probe the behavior of BPAPC on the molecular level.[1−20] However, several problems concerning the structure and mobility of BPAPC remain open: (i) conformational structure of the carbonate groups in the crystalline polymer; (ii) populations of the conformational states and nature of molecular motions in the glassy polymer; (iii) interchain orientational order in amorphous BPAPC.

According to a full helical parameter analysis supplemented by conformational energy calculations,[3] two idealized chain conformations with *cis*−*trans* and contracted *trans*−*trans* arrangement of the carbonate moiety are consistent with the fiber data of crystalline BPAPC given by Bonart.[2]

The relation of physical properties of glassy BPAPC (such as high impact strength below its glass transition temperature, T_g, of ∼150 °C) to some type of local molecular motion is generally accepted.[4,5] As the predominant molecular motion in BPAPC, 180° flips of the phenyl rings,[6−13] is energy conserving, short-range, mechanically active motion is best interpreted as a cooperative motion in BPAPC involving both the carbonate group and the phenyl rings.[5,14] The exact nature of the motions is determined by the barriers to internal rotations and the populations of the *cis*−*trans* and *trans*−*trans* conformations of the carbonate groups in amorphous BPAPC. According to the viscosity measurements of BPAPC in Θ-solvents[15] and X-ray analysis of low-molecular-weight model compounds of BPAPC,[3] the *trans*−*trans* conformations predominate in carbonate groups. Recently, this was supported by NMR experiments on glassy samples containing ^{13}C-labeled BPAPC,[16] indicating the *cis*−*trans* content lower than 10%. This finding is questioned by quantum-mechanical conformational calculations on model compounds[5,7,10] and by molecular simulations of BPAPC.[16−18] Three different molecular packings obtained with different construction methods and two force fields predict a typical *cis*−*trans* content of 25−30%.[16−18]

The NMR experiments with the deuterated and ^{13}C-labeled BPAPC samples show that glassy amorphous BPAPC consists on average of densely packed chains, and this result was interpreted in terms of the orientational order of locally parallel chain segments (bundles).[8,9] There is a controversy about the chain conformations in such ordered domains. Pietralla and Pieper[19] proposed locally ordered chains with various possible crystalline structures along a single chain. On the other hand, neutron scattering experiments indicate that crystalline-like chain conformations are not present in amorphous BPAPC.[20]

Infrared and Raman spectroscopy are useful tools to study conformations and conformational regularities in polymers; however, available experimental data on BPAPC are not conclusive.[21−26] In this article we present an analysis of infrared and Raman spectra of amorphous and semicrystalline BPAPC samples prepared by varying thermal and solvent treatment. Based on the found crystalline bands, the degree of crystallinity is determined and compared with the results of WAXS and DSC measurements. By using infrared and

S0024-9297(98)00762-1 CCC: $15.00
Published on Web 09/03/1998

Raman spectra and ab initio quantum mechanical calculations of diphenyl carbonate (DPC) as the model compound, an assignment of the bands conformationally sensitive to the *cis*−*trans* and *trans*−*trans* structures of the carbonate group is proposed. In some solvents (toluene, benzene), aggregation of BPAPC chains is observed, leading to ordered structures similar to those detected in crystalline BPAPC.

Experimental Section

Measurements. Infrared and Raman spectra were measured on a Bruker IFS-55 FT-IR spectrometer equipped with a Raman module FRA-106. Both infrared and Raman spectra were recorded at 2 cm^{-1} resolution and the Raman spectra were excited by a 1064 nm diode-pumped Nd:YAG laser with a power of 400 mW at a sample. Low-temperature infrared and Raman spectra were measured by means of an RIIC and Bruker variable temperature cell, respectively. For the measurements of the infrared spectra at elevated temperatures, a Perkin-Elmer heated cell was used.

Differential scanning calorimetry (DSC) measurements were performed using a Perkin-Elmer DSC-2 differential scanning calorimeter with a constant heating rate of 10 °C/min under a nitrogen atmosphere. Degrees of crystallinity were determined on the basis of the published data of enthalpy of fusion $\Delta H_f°$ for 100% crystalline BPAPC: 27.8 kJ/mol,[27] 33.5 kJ/mol.[28]

Wide-angle X-ray scattering (WAXS) patterns were obtained using a powder diffractometer HZG/4A of Freiberger Praezisionsmechanik GmbH (Germany). Cu Kα radiation was monochromatized with a Na filter and pulse-height analyzer, and diffracted radiation was recorded by means of a proportional counter. The degree of crystallinity in semicrystalline samples of BPAPC was calculated as the ratio of the integral intensity of the crystalline phase scattering to the total scattering intensity. The diffraction curve corresponding to the crystalline phase was obtained after separation of the amorphous component by making use of the scattering of completely amorphous BPAPC sample.

Samples. Polycarbonate samples were prepared from commercial-grade Bisphenol A polycarbonate SINVET 251 (ENI, Italy). The original BPAPC sample had a weight-average molecular weight (M_w) of 24 000 and a number-average molecular weight (M_n) of 9600, as measured by gel permeation chromatography. DSC and WAXS measurements indicated crystallinity lower than 0.5% for the original BPAPC samples. Only traces of crystallinity were observed in the samples obtained by annealing original pellets of BPAPC in a vacuum oven at 190 °C for 330 h.

Two types of semicrystalline samples of BPAPC were obtained by (i) dropwise precipitation from a chloroform solution (2% w/w) into pentane, slow evaporation of the solvents at room temperature, and subsequent heating at 80 °C for 64 h (BPAPC-1) and (ii) dropwise precipitation from a chloroform solution (2% w/w) into methanol, exposing the obtained powder to saturated vapors of acetone for 1 h, and subsequent annealing by heating in a vacuum oven at 190 °C for 4 h[8] (BPAPC-2).

The time dependence of the aggregation of BPAPC in solutions was studied by infrared spectroscopy. Prior to filling a KBr cell, solutions of BPAPC in toluene (0.5, 1.0, 2.0, and 4.0% w/w) and benzene (2% w/w) were homogenized in a sealed glass tube at 130 and 100 °C, respectively, for 1 h. Aggregated BPAPC in solution was used for preparation of another type of partially crystalline solid BPAPC. The sample BPAPC-3 was obtained from a homogenized BPAPC solution in toluene (2% w/w) kept at room temperature for 24 h. Thin films were prepared by room-temperature evaporation of the solvent from the gel. The rest of toluene was then removed by heating the sample at 100 °C for 1 h.

Infrared spectra of solid samples of BPAPC were first measured in KBr pellets. As the presence of KBr in the pellets tends to modify the molecular structure of BPAPC (as will be discussed later), another set of samples for infrared measurements were prepared in the form of thin films cast from a chloroform solution on the KBr window. The residual solvent was removed by heating at 90 °C for 1 h. A semicrystalline sample of BPAPC suitable for infrared analysis was prepared by annealing a thin film on the KBr window in a vacuum oven at 190 °C for 330 h (BPAPC-4).

Calculations. The calculations were run on SGI workstations using the Gaussian 94 program package.[29] Molecular structures of diphenyl carbonate were studied at the DFT level using B3LYP functional;[30−32] the basis set was of 6-31G(d) quality. The calculations were performed in C_1 symmetry, the geometries were fully optimized and the stationary states were verified by inspecting their Hessian. Zero-point energy and thermal energy corrections were included in calculations of thermodynamic quantities (enthalpy H and Gibbs energy $G = H - TS$). Solvent effects were determined by self-consistent reaction field calculations with the Onsager model.[33,34] This model assumes the solute as a cavity of a given shape, which is surrounded by a polarizable continuous medium with permittivity ϵ.

Results and Discussion

Conformational Analysis of the Diphenyl Carbonate Moiety. Predominant molecular motions in BPAPC, 180° flips of the phenyl rings, proceed between two structurally and spectroscopically identical conformations, and thus the *trans*−*trans* and *cis*−*trans* conformational states of the carbonate group are expected to be the only spectroscopically distinguished conformations in BPABC. In previous studies of a model compound, diphenyl carbonate (DPC), conformationally sensitive bands were revealed in the infrared spectra.[22,35,36] Temperature dependence of infrared spectra of a DPC solution in CCl_4 showed that in the doublet at 1240 and 1227 cm^{-1}, the band at 1240 cm^{-1} corresponds to the energetically more favored conformation[22] stabilized by the enthalpy difference of 1.1 kcal/mol. According to the ab initio calculations,[7,17] the *trans*−*trans* structure is energetically preferred (by 2.74 kcal/mol with the 6-31G(d) basis set[7]), and this result has been accepted in recent studies on glassy BPAPC.

To get more insight into the conformational behavior of the diphenyl carbonate moiety, we have investigated infrared and Raman spectra of DPC in solutions with different permittivities (Figure 2). In addition to the carbonyl band, which is complicated by Fermi resonance,[35,36] and the doublet at 1015 and 997 cm^{-1}, which is observed only in the Raman spectra, considerable spectral changes occur in the region of the C−O−C stretching vibrations, both in infrared and Raman spectra (Figure 2). In the case of the $CDCl_3$ solution, a doublet at 1249 and 1234 cm^{-1} occurs in the infrared spectrum and at 1240 and 1228 cm^{-1} in the Raman spectrum. The bands shown in Figure 2 exhibit frequency shifts due to the changed permittivity of the environment. Nevertheless, it is evident from Figure 2 that with increasing permittivity ϵ, the intensity of the high-frequency component of the doublet increases in the infrared spectra whereas the intensity of the low-frequency component increases in the Raman spectra. As these changes in relative band intensities are analogous to the effects observed in temperature dependences of DPC solutions in CCl_4[22] and chloroform (Figure 3), they can be also attributed to conformational transitions between the *trans*−*trans* and *cis*−*trans* structures of the carbonate group. Different behavior of the bands in the infrared and Raman spectra is explained by the fact that from two fundamental modes dominated by C−O−C stretching vibrations of the

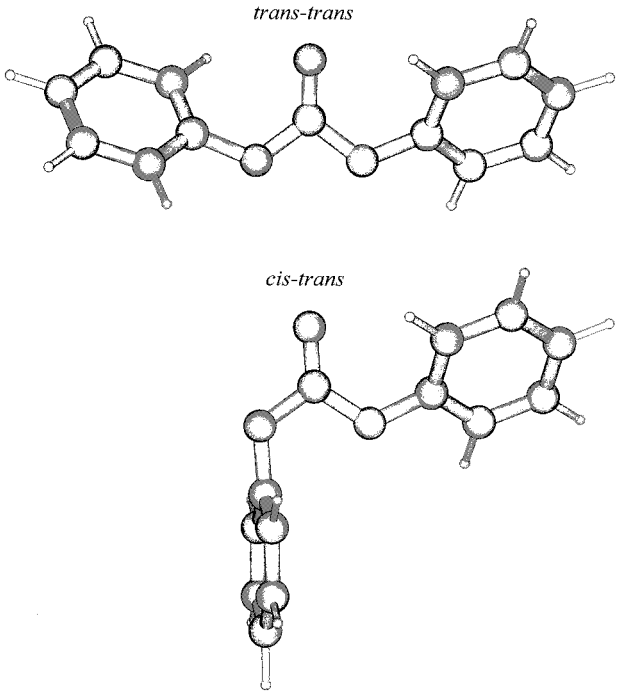

Figure 1. DFT-optimized (at the B3LYP/6-31G(d) level) *trans*−*trans* and *cis*−*trans* conformational structures of diphenyl carbonate.

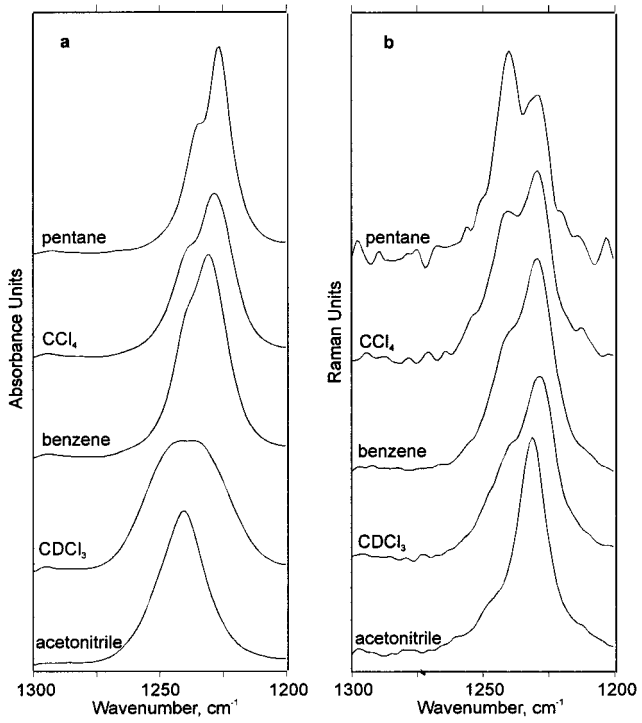

Figure 2. Infrared (a) and Raman (b) spectra of DPC solutions in pentane ($\epsilon = 1.84$), tetrachloromethane ($\epsilon = 2.23$), benzene ($\epsilon = 2.27$), $CDCl_3$ ($\epsilon = 4.71$), and acetonitrile ($\epsilon = 35.7$). Spectra of the solvents are subtracted.

carbonate group, the symmetric mode is predominantly active in the Raman spectra while the asymmetric mode is predominant in the infrared spectra. According to the calculations at the HF/6-31G(d) level, the intensity of the complementary, less intensive mode is at least 1 order lower in both the infrared and Raman spectra, and therefore, in the further analysis, their contributions in the spectra are neglected for simplicity reasons.

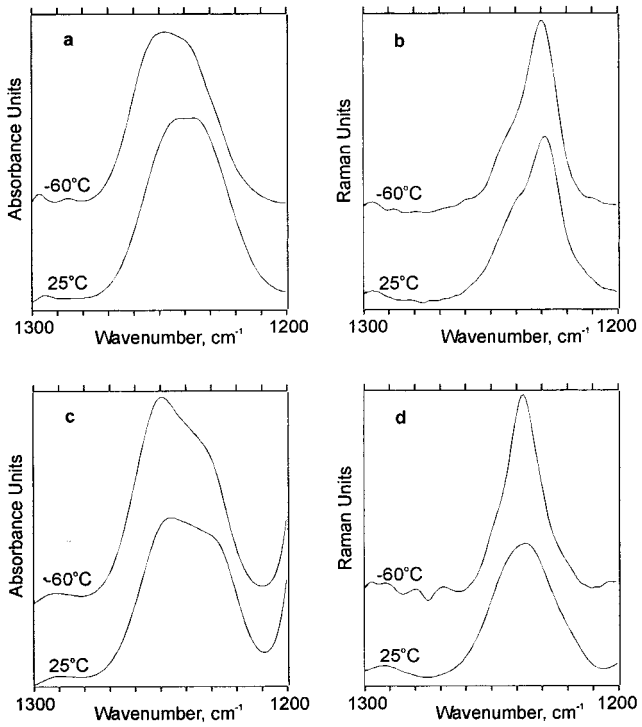

Figure 3. Temperature dependence of infrared (a, c) and Raman (b, d) spectra of DPC (a, b) and BPAPC (c, d) solutions in $CDCl_3$. Spectra of the solvents are subtracted.

We have calculated structural and thermodynamic parameters for the *trans*−*trans* and *cis*−*trans* conformational states of DPC by semiempirical (AM1) and ab initio methods (Figure 1 and Table 1). Two main conclusions can be made from the data presented in Table 1: (1) The relatively high energy preference of the *trans*−*trans* structure obtained in the ab initio calculations at the Hartree−Fock level (6-31G(d) basis set) is considerably lowered when electron correlation is included in the quantum mechanical calculations, either by using Møller−Plesset perturbation theory[38,39] (MP2) or density functional theory[40] (DFT). As the ratio of the conformer populations is governed by the difference of the Gibbs energies, ΔG, it is evident from Table 1 that by including thermal effects, the conformer equilibrium is further shifted to a higher content of the *cis*−*trans* structure. These trends in the results of the theoretical calculations indicate that the Gibbs energy difference between the *cis*−*trans* and *trans*−*trans* structures is very small, in agreement with the data obtained from infrared spectroscopy.[22] Taking into account the accuracy of quantum mechanical calculations at an accessible level, the theoretically predicted preference of the *trans*−*trans* conformer at room temperature can be questioned. (2) Nonspecific solvent−solute interactions incorporated in the calculations by means of the permittivity ϵ of the continuous environment cause a relative decrease in the energy of the *cis*−*trans* structure. This is in agreement with the empirical rule that the conformational structure with a higher electric dipole moment is preferred in the environment with a higher permittivity. According to the calculations at the B3LYP/6-31G(d) level, the dipole moment of DPC is 0.28 D for the *trans*−*trans* structure and 3.44 D for the *cis*−*trans* structure.

On the basis of all the results given above, we assume that in the C−O−C stretching region of the vibrational

Table 1. Energy, Enthalpy, and Gibbs Energy Differences and Rotational Energy Barrier between the *Cis*−*Trans* and *Trans*−*Trans* Conformational States of Diphenyl Carbonate

method	environment	ΔE,[a] kcal/mol	ΔH_{298},[b] kcal/mol	ΔG_{298},[c] kcal/mol	barrier,[d] kcal/mol
AM1			0.15		2.89
HF/6-31G(d)	gas phase	2.76	2.66	2.66	6.91
B3LYP/6-31G(d)	gas phase	2.27	2.14	1.79	6.62
B3LYP/6-31G(d)	pentane,[e] $\epsilon = 1.84$	1.94	1.81	1.46	6.48
B3LYP/6-31G(d)	BPAPC,[e] $\epsilon = 2.92$	1.77	1.64	1.29	6.40
B3LYP/6-31G(d)	acetonitrile,[e] $\epsilon = 35.7$	1.38	1.25	0.90	6.23
MP2/6-31G(d)//HF/6-31G(d)	gas phase	1.89			7.16
MP2/6-31G(d)//HF/6-31G(d)	acetonitrile,[e] $\epsilon = 35.7$	1.04			6.73

[a] $\Delta E = E_{cis-trans} - E_{trans-trans}$. [b] Ab initio enthalpy difference at 298.15 K obtained from ΔE by means of zero-point energy and thermal energy corrections ($\Delta H = \Delta E + \Delta E(\mathrm{ZPE}) + \Delta E_{vib} + \Delta E_{transl} + \Delta E_{rot}$). [c] Gibbs energy difference ($\Delta G = \Delta H - T\Delta S$, where ΔS is the calculated entropy difference) at 298.15 K. [d] Rotational energy barrier about the O−CO bond calculated with respect to the *Trans*−*Trans* conformation. [e] Permittivity taken from the ref 37.

spectra of DPC (1200−1300 cm^{-1}), the high-frequency component in the infrared spectra and the low-frequency component in the Raman spectra can be assigned to the *cis*−*trans* conformational structure. From the temperature dependences of the infrared and Raman spectra of DPC in $CDCl_3$ (Figure 3) and of the infrared spectra of DPC in CCl_4,[22] it follows that the *cis*−*trans* structure is energetically preferred in these solutions. The behavior of relative intensities of the bands in the C−O−C stretching region in the spectra of measured solutions and in temperature dependences of $CDCl_3$ solutions of BPAPC and DPC is analogous. Therefore, it can be assumed that the obtained information about the conformational structure of the carbonate moiety in DPC can be transferred to BPAPC.

Analysis of the ratios of band intensities in the 1200−1300 cm^{-1} region of the infrared and Raman spectra of DPC measured in various solutions at different temperatures suggests that the infrared integrated absorptivity of the asymmetric C−O−C stretching mode is higher for the *trans*−*trans* structure. This is supported by the results of quantum mechanical calculations of infrared absorptivities. At the B3LYP/6-31G(d) level, infrared integrated absorptivity of the asymmetric C−O−C stretching mode in DPC is 1.86×10^6 m/mol for the *trans*−*trans* structure and 1.12×10^6 m/mol for the *cis*−*trans* structure. The observed ratios of the band intensities in the C−O−C stretching region of infrared spectra of amorphous BPAPC (Figure 4) thus indicate a high population (preference) of the *cis*−*trans* structure at room temperature. In Figure 4 it is seen that the intensity ratio of the conformationally sensitive bands in the infrared spectra changes in the whole measured temperature range. Observed spectroscopic effects are reversible on the time scale of performed experiments; the samples were cooled and heated with the rate ∼100 °C/h. This suggests that populations of the carbonate conformations can change reversibly even far below the glass transition temperature ($T_g \sim 150$ °C). These findings support the conclusions of the recent ^{13}C NMR work[16] that structural rearrangements at the carbonate−phenylene units might take place so that the local thermodynamic equilibrium in the glass can be approached. The mechanical secondary relaxation behavior indicates that substantial intramolecular cooperative motion is extended to about 5−7 repeat units.[41−43] Using the above given assignments of vibrational bands to the respective conformers of BPAPC, it can be concluded that the content of the *cis*−*trans* conformation of the carbonate group increases with decreasing temperature. With respect to the continuing discussion[16−18] concerning the content of different carbonate conformations in amorphous BPAPC, these results support

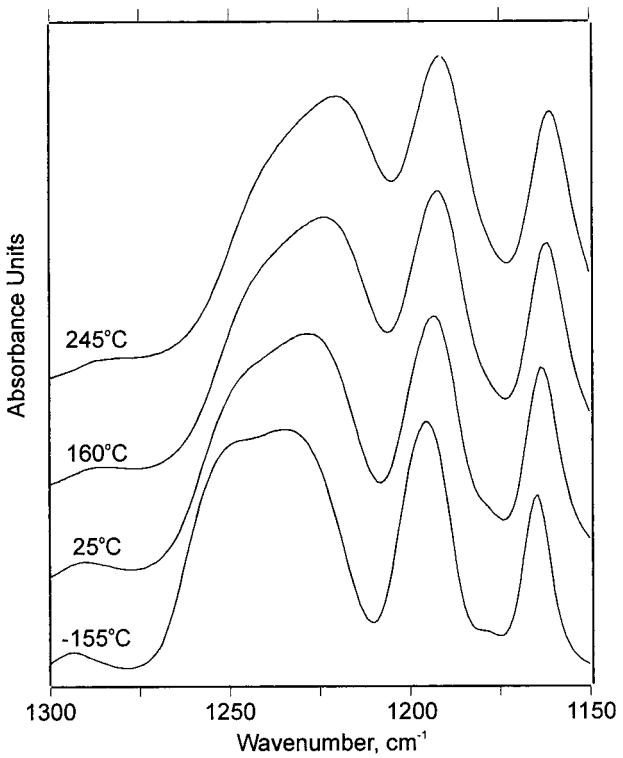

Figure 4. Temperature dependence of infrared spectra of an amorphous BPAPC film on the KBr window.

indications of molecular simulations[17,18] that the content of the *cis*−*trans* structure is higher than it follows from NMR experiments.[16]

Partially Crystalline BPAPC. From Figure 5 it can be seen that the Raman spectrum of the partially crystalline BPAPC considerably differs from the spectrum of the original amorphous sample in several regions. Changes in the band intensities and wavenumbers are more pronounced in the spectrum of pure crystalline BPAPC (Figure 5D) obtained from the spectrum of the partially crystalline sample (Figure 5C) by subtraction of the spectrum of pure amorphous BPAPC (Figure 5A) multiplied by the factor 0.59. The factor was chosen so that the counterpeaks resulting from the subtracted peaks corresponding to the pure amorphous form are minimized. The main differences detected in the Raman spectra of BPAPC due to the transition from the amorphous to the crystalline state can be found in the carbonyl band region (shift from 1775 to 1767 cm^{-1}) and in the region corresponding to the stretching vibrations of the C−O−C group (the band at 1235 cm^{-1} is shifted to 1248 cm^{-1} with shoulders at 1237 and 1220

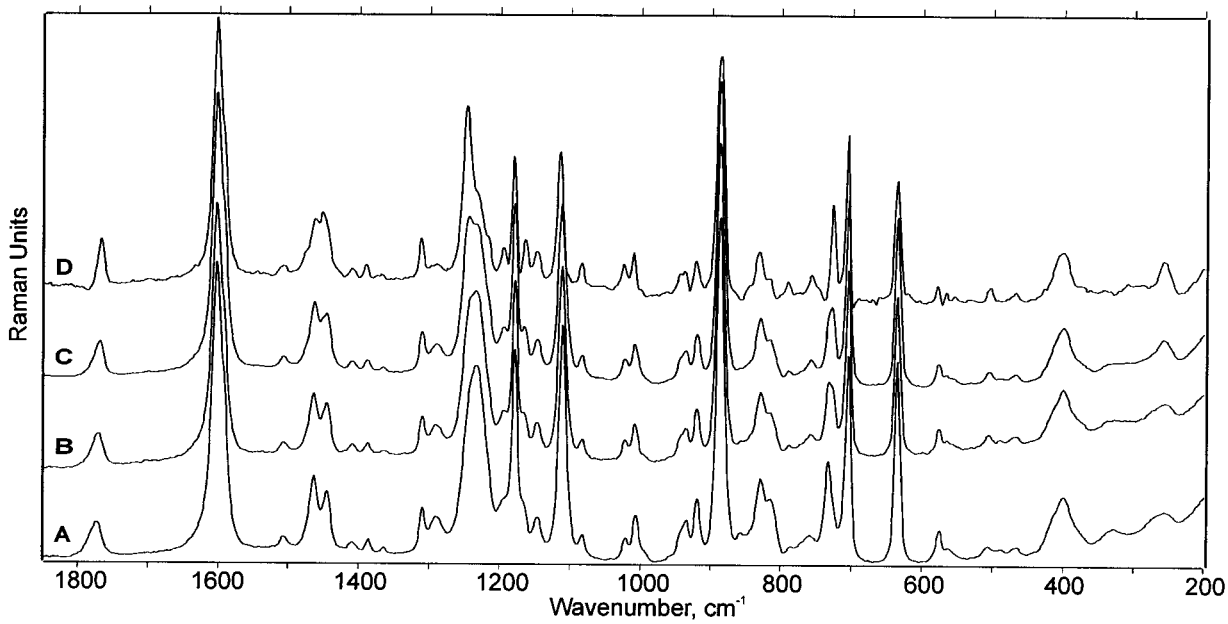

Figure 5. Raman spectra of BPAPC: (A) original BPAPC sample; (B) powder obtained by precipitation from a chloroform solution into methanol, exposed to saturated acetone vapors for 1 h and annealed at 190 °C for 4 h; (C) powder obtained by precipitation from a chloroform solution into pentane and annealed at 80 °C for 64 h; (D) normalized difference spectrum obtained by subtracting spectrum A (multiplied by the factor 0.59) from spectrum C.

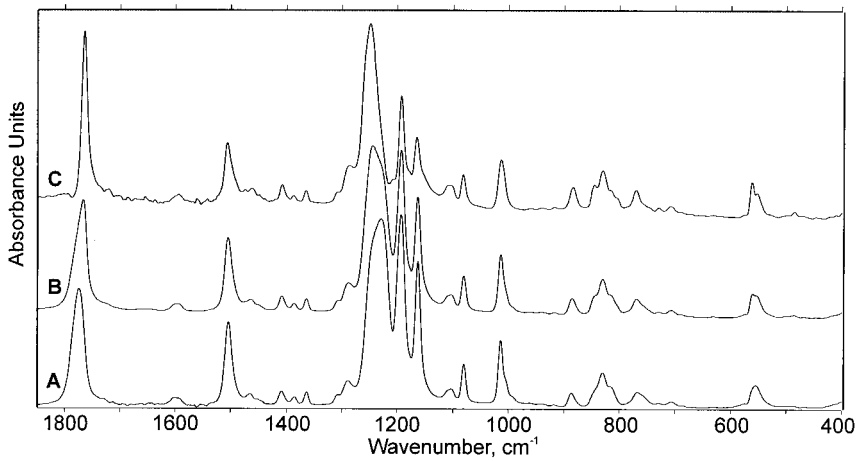

Figure 6. Infrared spectra of BPAPC: (A) a film cast from a chloroform solution on the KBr window; (B) sample A annealed in a vacuum at 190 °C for 330 h; (C) normalized difference spectrum obtained by subtracting spectrum A (multiplied by the factor 0.65) from spectrum B.

cm^{-1}). The band at 735 cm^{-1} in the amorphous form is shifted to 728 cm^{-1} in the crystalline form.

Analogous differences between the amorphous and crystalline forms of BPAPC are detected in the infrared spectra of BPAPC films on KBr windows (Figure 6). The spectrum of pure crystalline BPAPC (Figure 6C) was obtained from the spectrum of the partially crystalline sample (Figure 6B) by subtraction of the spectrum of pure amorphous BPAPC (Figure 6A) multiplied by factor 0.65. Compared with the amorphous form, the carbonyl band in the spectrum of crystalline BPAPC is shifted from 1775 to 1765 cm^{-1}, the doublet at 1229 and 1240 cm^{-1} in the region of the asymmetric C−O−C stretching vibration is transferred to a band at 1251 cm^{-1} with a shoulder at 1261 cm^{-1}, and the intensity of the band at 564 cm^{-1} is much increased.

Figure 7 shows infrared spectra of BPAPC samples in KBr pellets. The spectrum of the original sample of amorphous BPAPC in the KBr pellet (Figure 7A) is very similar to the spectrum of amorphous BPAPC in the form of a thin film (Figure 6A). Optical effects due to the inhomogeneities of BPAPC in the KBr pellet cause the only differences manifested in the relative intensities and shapes of the strong bands. In infrared spectra of the originally partially crystalline samples BPAPC-1 and BPAPC-2 (Table 2) measured in KBr pellets, no crystalline bands are observed (Figure 6C) and the spectra are indistinguishable from the spectrum of the amorphous BPAPC sample shown in Figure 7A. This demonstrates that grinding and pressing the partially crystalline BPAPC sample with KBr tends to destroy the crystalline structure of the polymer. On the other hand, crystalline bands in the spectrum of the melted and subsequently slowly cooled KBr pellet kept in the Perkin-Elmer heated cell (Figure 7C) indicate some degree of crystallinity. According to the DSC measurements, the crystallinity of the pure BPAPC sample obtained from this KBr pellet by removing KBr with water is ∼3%. The crystallinity is induced by the presence of the KBr matrix, as no crystallinity was

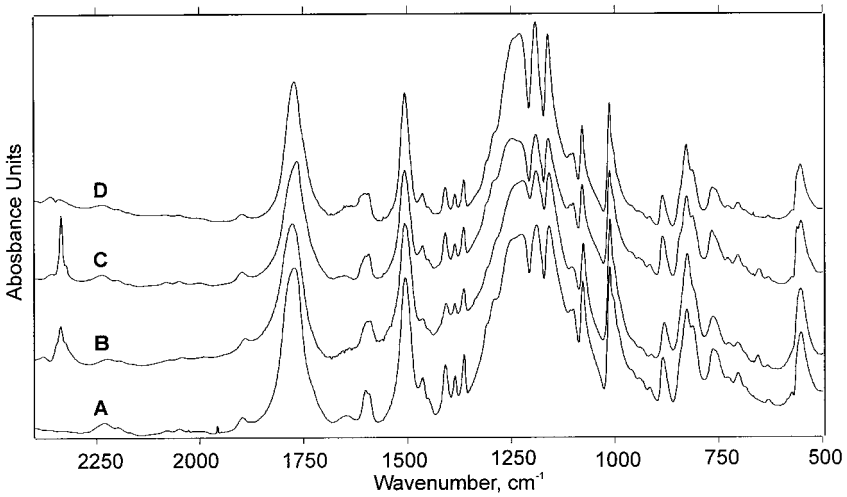

Figure 7. Infrared spectra of semicrystalline BPAPC in KBr pellets measured successively at 25 °C (A), 245 °C (B), and 25 °C (C, D). For the measurement of spectrum D, a new KBr pellet was prepared from sample C by new grinding and pressing.

Table 2. Degrees of Crystallinity (in %) of the BPAPC Samples

				Raman[b]		
sample	treatment	WAXS	DSC[a]	735 cm^{-1}	1235 cm^{-1}	infrared
BPAPC-1	dissolved in $CHCl_3$, precipitated into pentane, annealed at 80 °C (64 h)	32	20 (24)	41	25	
BPAPC-2	dissolved in $CHCl_3$, precipitated into methanol, acetone vapors, annealed at 190 °C (4 h)	29	14 (17)	32	15	
BPAPC-3	room-temperature evaporation of the solvent from the gel in toluene	36	17 (20)	39	16	41
BPAPC-4	dissolved in $CHCl_3$, cast, and annealed at 190 °C (330 h)		19 (23)			35

[a] Based on enthalpy of fusion of 33.5 kJ/mol[28] (27.8 kJ/mol[27]) for the 100% crystalline polymer. [b] By spectral subtraction using characteristic amorphous bands at 735 and 1235 cm^{-1} (see the text).

observed in pure films of BPAPC undergoing the same temperature cycle. This stimulation of crystallization of BPAPC in the presence of ions is analogous to the crystallization induced by organic salts.[44] The sharp peak at 2335 cm^{-1} detected in the spectra of melted and cooled samples (Figure 7B,C) corresponds to the stretching vibration of CO_2, and its presence indicates degradation of BPAPC. The band originates from CO_2 molecules, which are bound in the solid matrix of the KBr pellet and can be released by grinding and pressing a new pellet (see Figure 7D).

Taking into account the changes of the band shapes and intensities observed in the infrared and Raman spectra of BPAPC in the amorphous state and in solution as a consequence of changes in populations of chain conformations, it is clear that the differences between the spectra of the amorphous and crystalline forms of BPAPC (Figures 5 and 6) are caused predominantly by intrachain and interchain interactions in the crystalline polymer. The C═O and C−O−C stretching modes have large transition dipole moments, as is evident from their infrared intensities. Considerable band shifts or band splittings in the carbonyl stretching and C−O−C stretching regions can thus be explained by strong resonance transition dipole−transition dipole interactions[45] of the closely ordered carbonate groups in the crystalline cell. (The C═O stretching mode is probably also affected by the Fermi resonance.[22]) As the distance of the carbonate groups in the neighboring monomer units of a BPAPC chain is large (0.9−1.2 nm[20]), a significant contribution to the splitting must originate from the interaction of the spatially close carbonate groups either from different chains or from remote monomer units in one chain. These effects obscure changes in band intensities that correspond to conformational transitions. Therefore, using available spectroscopic data, it is not possible to decide which conformational structure of the carbonate group is present in the crystalline form. Characteristic crystalline bands at 728 cm^{-1} in the Raman spectra and 560 cm^{-1} in the infrared spectra, corresponding to the localized skeletal vibrations, are probably related to the regular ordering along the chain. Such characteristic bands appear in the spectra if long enough regular sequences are present in the sample; frequency shifts due to the presence of *all-trans* sequences in the case of polyethylene were investigated by Snyder.[46]

As was described above, using the spectrum of pure amorphous BPAPC, the spectrum of the crystalline polymer can be obtained from the spectrum of a partially crystalline sample by spectral subtraction (Figures 5 and 6). The same method was used for the determination of the pure amorphous form content in the sample. In the case of the sample BPAPC-4, the same polymer film was used in measurements of the infrared spectra of amorphous and partially crystalline samples and the overall absorbance was not changed by crystallization (Figure 6). Therefore, the multiplication factor in the spectral subtraction gives directly the amorphous form content in the crystallized sample. In other cases, absorbances or Raman intensities of the bands in the spectra of different samples were not directly comparable and they had to be normalized before subtraction. A scaling factor was therefore applied to each spectrum. It was derived as a mean value of the integrated intensities of several bands that were found to be unaffected by crystallization (bands at 3074 and 889 cm^{-1} in the Raman spectra and the C−H stretching region 3100−2800 cm^{-1} in the infrared spectra). Complements to the amorphous form content, considered to be

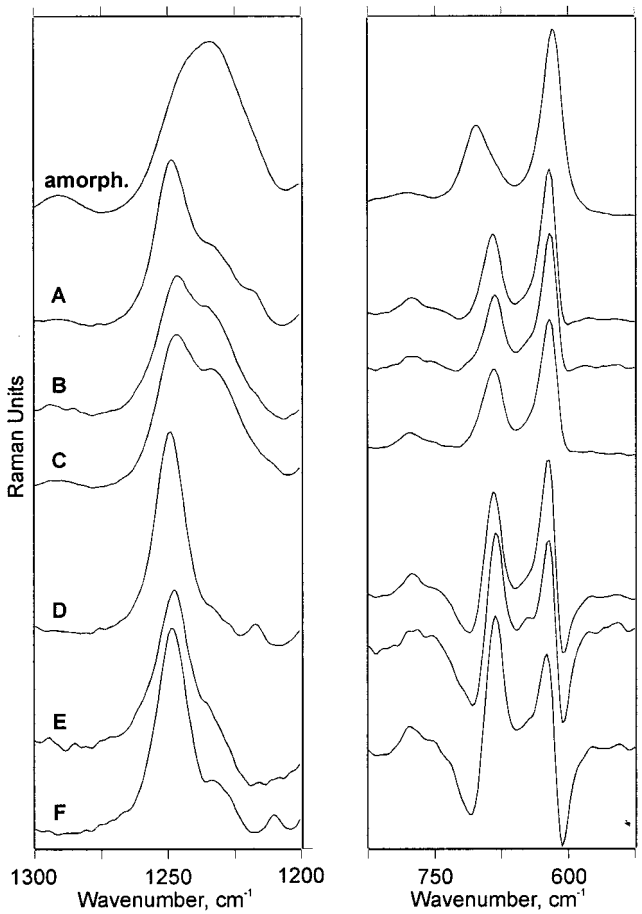

Figure 8. Difference Raman spectra obtained by subtracting the spectrum of amorphous BPAPC from the spectra of semicrystalline samples BPAPC-1 (A, D), BPAPC-2 (B, E), and BPAPC-3 (C, F). Factors were chosen so as to compensate amorphous bands either at 735 cm^{-1} (A, 0.59; B, 0.68; C, 0.61) or at 1235 cm^{-1} (D, 0.75; E, 0.85; F, 0.84).

the values of crystallinity derived by means of Raman and infrared spectroscopy are given in Table 2.

From Table 2 it follows that the degrees of crystallinity in the partially crystalline BPAPC samples determined by WAXS are significantly higher compared with the data obtained by DSC. Degrees of ordering obtained from the infrared and Raman spectra by spectral subtraction performed so that no counterpeaks appear in the whole resulting spectrum (for the Raman spectra, column 735 cm^{-1} in Table 2) are relatively high, and they are close to the WAXS values of crystallinity. Details of the difference Raman spectra are shown in Figure 8. It can be seen that while the characteristic amorphous band at 735 cm^{-1} is well compensated for all three samples BPAPC-1, BPAPC-2, and BPAPC-3 (spectra A, B, and C), relatively strong bands are present at the position of the amorphous bands in the C−O−C stretching region (1235 cm^{-1}). The fact that intensities of the 1235 cm^{-1} bands in the difference spectra of samples BPAPC-1, BPAPC-2, and BPAPC-3 are significantly different indicates that at least part of the Raman intensity corresponds to the noncompensated amorphous bands. The difference spectra D, E, and F in Figure 8 were obtained under the assumption that no intensive Raman bands in the spectra of crystalline BPAPC occur at frequencies close to 1235 cm^{-1}. It can be seen in Table 2 that corresponding degrees of ordering are close to the values of crystallinity determined by DSC. We think that differences between the values of ordering assessed from the Raman spectra using the bands at 735 and 1235 cm^{-1} follow from different requirements for the regularities that cause the observed band shifts or splittings. As was discussed above, the shift of the amorphous band at 735 cm^{-1} to 728 cm^{-1} corresponds to the formation of sufficiently long one-dimensional regular chain sequences in the sample. On the other hand, splitting of the C−O−C stretching modes is caused by the transition dipole coupling, which requires a regular interchain arrangement in the crystalline cell of BPAPC. The determined values of crystallinity shown in Table 2 thus indicate that in semicrystalline samples of BPAPC, the contents of polymer chains with regular intrachain arrangement are considerably higher compared with the content of perfect three-dimensional crystalline regions. The values of crystallinity given in Table 2 suggest that the requirements for the extent of the long-range order of the chains in samples of semicrystalline BPAPC are less strict for the X-ray crystalline reflections compared with the DSC enthalpies of melting. The observed differences in the contents of regions with intrachain and interchain regular arrangements in semicrystalline BPAPC are probably related to the interfacial region between the crystalline and amorphous phases characterized by partial ordering of the chain units. Experimental studies clearly demonstrate the existence of such a third phase in polyethylene.[47−49]

Aggregation of BPAPC in Solution. BPAPC is hardly soluble in solvents such as toluene or benzene and transparent homogeneous solutions could be prepared only by 1-h heating samples in sealed glass tubes at high temperature (∼130 °C for toluene and ∼110 °C for benzene solutions). After cooling the sample to room temperature, gradual aggregation of the polymer is observed and finally an opaque homogeneous gel is formed. The aggregation begins after a time delay; for the measured solutions, it was observed in the range from 3 min (4% w/w solution in toluene) to 4 days (2% w/w solution in benzene). On heating the samples to approximately 125 (toluene) or 100 °C (benzene), the gels can be converted back to the original transparent solution. In the case of BPAPC solutions, to our knowledge, such gelation has not been reported before; however, it is analogous to the thermoreversible gelation observed with several other synthetic polymers.[50]

In infrared spectra, the increasing intensity of characteristic bands at 1765 and 1250 cm^{-1} (Figure 9) and the band at 560 cm^{-1} manifests the gel formation of BPAPC in solution. Analogous spectroscopic effects are characteristic of the crystalline form of BPAPC (Figure 6). This suggests that observed aggregation of BPAPC in solution leads to crystalline-like chain arrangements. As all changes in BPAPC spectra during the aggregation proceed in a parallel way, we suppose that both the conformational arrangement along the chains and the interchain arrangements in solution occur simultaneously. Overlapping bands in the carbonyl stretching region were separated by the least-squares method into two components at 1777 and 1765 cm^{-1} and their integrated intensities were used for the calculation of the relative content of the aggregated polymer as the ratio $A_{1765}/(A_{1765} + A_{1777})$. Neglecting the differences in integrated absorptivities of carbonyl stretching vibrations in the aggregated and nonaggregated forms of BPAPC is justified by the fact that the total integrated

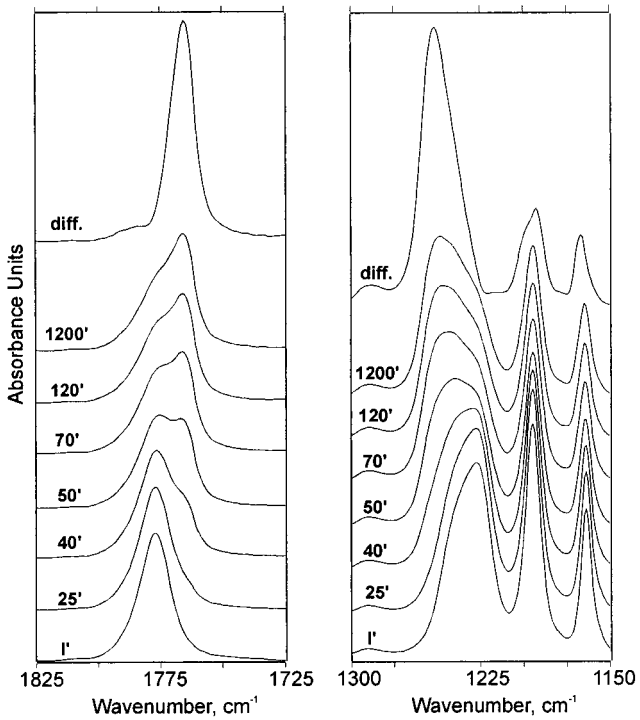

Figure 9. Time dependence of infrared spectra of a toluene BPAPC solution (1% w/w) measured at room temperature immediately after homogenizing at 130 °C. Normalized difference spectrum was obtained by subtracting the initial spectrum (1′) (multiplied by the factor 0.48) from the final spectrum (1200′). The spectrum of the solvent was subtracted.

absorbance of the carbonyl stretching region is changed only by a few percent during aggregation.

Graphs shown in Figure 10 demonstrate that the rate of the BPAPC aggregation in toluene is decreasing and the time delay before the start of the aggregation is increasing with decreasing concentration of the solution. These results indicate that the kinetics of the polymer aggregation is driven primarily by intermolecular arrangements of the chains. In the measured range of concentrations (0.5−4.0% w/w), the limiting value for the portion of the aggregated BPAPC in toluene does not depend on the concentration of solution and is approximately the same for the measured benzene solution of BPAPC (2% w/w). The limiting value of aggregation makes ∼47% according to the results of band deconvolution (Figure 10) and ∼52% according to spectral subtraction (Figure 8). Both values are higher compared with the degree of crystallinity of all the measured samples of partially crystalline solid BPAPC (Table 2). By the room temperature evaporation of the solvent from the gel, a partially crystalline sample of BPAPC with a high degree of crystallinity is obtained (BPAPC-3 in Table 2).

Conclusions

Based on the spectroscopic analysis and ab initio quantum mechanical calculations of DPC, assignment of the infrared and Raman bands to the *trans*−*trans* and *cis*−*trans* structures of the carbonate moiety is proposed. Analysis of the spectra indicates that the *cis*−*trans* conformation is energetically favored both in BPAPC solutions and in amorphous BPAPC and that the *cis*−*trans* structure content can be increased with decreasing temperature even below the glass transition temperature T_g of the amorphous glassy BPAPC.

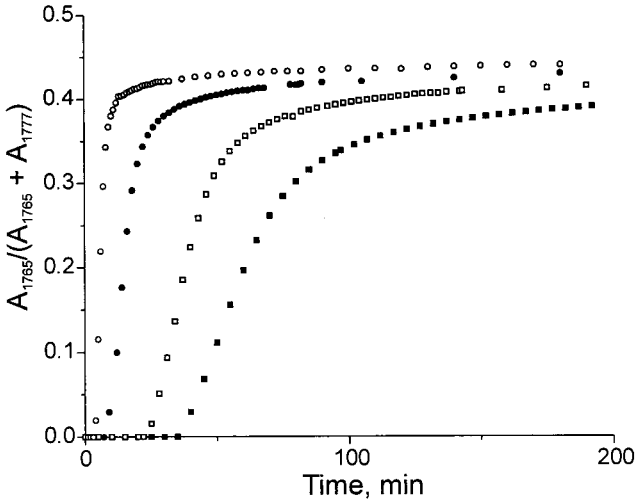

Figure 10. Time dependence of BPAPC aggregation in toluene solutions of different concentrations ((■) 0.5%; (□) 1%; (●) 2%; (○) 4%) determined from the infrared spectra measured at room temperature immediately after homogenizing at 130 °C.

Studies of several samples of semicrystalline BPAPC obtained by varying thermal and solvent treatment show that the values of crystallinity determined by WAXS are considerably higher compared with those obtained with DSC. The observed differences can be related to the degrees of ordering as determined by characteristic Raman bands at 735 and 1235 cm^{-1}, which are predominantly sensitive to the intrachain and interchain ordering, respectively. These effects are probably associated with the partial ordering in the interfacial region between the crystalline and amorphous phases.

In some solvents (toluene, benzene), aggregation of BPAPC occurs, leading to the gel with molecular structures of BPAPC analogous to that observed in the crystalline phase of semicrystalline BPAPC samples. The chain arrangement is preserved in the solid, partially crystalline samples obtained by the room-temperature evaporation of the solvent from the gel.

Acknowledgment. The authors thank the Grant Agency of the Czech Republic for financial support (Grants No. 203/97/0539 and 106/97/1071).

References and Notes

(1) Prietschk, A. *Kolloid-Z.* **1958**, *156*, 8.
(2) Bonart, R. *Makromol. Chem.***1966**, *92*, 149.
(3) Perez, S.; Scaringe, R. P. *Macromolecules* **1987**, *20*, 68.
(4) Schaefer, J.; Stejskal, E. O.; Steger, T. R.; Sefcik, M. D.; McKay, R. A. *Macromolecules* **1980**, *13*, 1121.
(5) Henrichs, P. M.; Luss, H. R.; Scaringe, R. P. *Macromolecules* **1989**, *22*, 2731.
(6) Schaefer, J.; Stejskal, E. O.; Perchak, D.; Skolnick, J.; Yaris, R. *Macromolecules* **1985**, *18*, 368.
(7) Laskowski, B. C.; Yoon, D. Y.; McLean, D.; Jaffe, R. L. *Macromolecules* **1988**, *21*, 1629.
(8) Lee, P. L.; Kowalewski, T.; Poliks, M. D.; Schaefer, J. *Macromolecules* **1995**, *28*, 2476.
(9) Klug, C. A.; Zhu, W.; Tasaki, K.; Schaefer, J. *Macromolecules* **1997**, *30*, 1734.
(10) Bicerano, J.; Clark, H. A. *Macromolecules* **1988**, *21*, 585.
(11) Henrichs, P. M.; Nicely, V. A. *Macromolecules* **1990**, *23*, 3193.
(12) Henrichs, P. M.; Nicely, V. A. *Macromolecules* **1991**, *24*, 2506.
(13) Klug, C. A.; Wu, J.; Xiao, C.; Yee, A. F.; Schaefer, J. *Macromolecules* **1997**, *30*, 6302.
(14) Jones, A. A. *Macromolecules* **1985**, *18*, 902.
(15) Williams, A. D.; Flory, P. J. *J. Polym. Sci., Polym. Phys. Ed.* **1968**, *6*, 1945.

(16) Tomaselli, M.; Zehnder, M. M.; Robyr, P.; Grob-Pisano, C.; Ernst, R. R.; Suter U. W. *Macromolecules* **1997**, *30*, 3579.
(17) Hutnik, M.; Argon, A. S.; Suter U. W. *Macromolecules* **1991**, *24*, 5956.
(18) Hutnik, M.; Gentile F. T.; Ludovice P. J.; Suter U. W.; Argon, A. S. *Macromolecules* **1991**, *24*, 5962.
(19) Pietralla, M.; Pieper, T. *Colloid Polym. Sci.* **1990**, *268*, 797.
(20) Cervinka, L.; Fischer, E. W.; Dettenmaier, M. *Polymer* **1991**, *32*, 12.
(21) Kulczycki, A. *Spectrochim. Acta* **1985**, *41A*, 1427.
(22) Schmidt, P.; Dybal, J.; Turska, E.; Kulczycki, A. *Polymer* **1991**, *32*, 1865.
(23) Stuart, B. H. *Polym. Bull.* **1996**, *36*, 341.
(24) Heymans, N. *Polymer* **1997**, *38*, 3435.
(25) Hopfe, I.; Pompe, G.; Eichhorn, K.-J. *Polymer* **1997**, *38*, 2321.
(26) Brunelle, D. J.; Gerbauskas, M. F. *Macromolecules* **1993**, *26*, 2724.
(27) Mercier, J. P.; Legras, R. *J. Polym. Sci., Polym. Lett. Ed.* **1970**, *8*, 645.
(28) Wunderlich, B.; Cheng, S. Z. D.; Loufakis K. Thermodynamic Properties of Polymers. *Encyclopedia of Polymer Science and Engineering*; Wiley: New York, 1989; Vol. 16, p 778.
(29) Frisch, M. J.; Trucks, G. W.; Schlegel, H. B.; Gill, P. M. W.; Johnson, B. G.; Robb, M. A.; Cheeseman, J. R.; Keith, T.; Petersson, G. A.; Montgomery, J. A.; Raghavachari, K.; Al-Laham, M. A.; Zakrzewski, V. G.; Ortiz, J. V.; Foresman, J. B.; Cioslowski, J.; Stefanov, B. B.; Nanayakkara, A.; Challacombe, M.; Peng, C. Y.; Ayala, P. Y.; Chen, W.; Wong, M. W.; Andres, J. L.; Replogle, E. S.; Gomperts, R.; Martin, R. L.; Fox, D. J.; Binkley, J. S.; Defrees, D. J.; Baker, J.; Stewart, J. P.; Head-Gordon, M.; Gonzalez, C.; Pople, J. A. *Gaussian 94, Revision E.2*; Gaussian, Inc.: Pittsburgh, PA, 1995.
(30) Becke, A. D. *J. Chem. Phys.* **1993**, *98*, 1372.
(31) Stephens, P. J.; Delvin, F. J.; Chabalowski, C. F.; Frisch, M. J. *J. Phys. Chem.* **1994**, *98*, 11623.
(32) Lee, C.; Yang, W.; Paar, R. G. *Phys. Rev.* **1993**, *B 37*, 785.
(33) Onsager, L. *J. Am. Chem. Soc.* **1936**, *58*, 1486.
(34) Wong, M. W.; Frisch, M. J.; Wiberg, K. B. *J. Am. Chem. Soc.* **1991**, *113*, 4776.
(35) Oki, M.; Nakanishi, H. *Bull. Chem. Soc. Jpn* **1971**, *44*, 3419.
(36) Guiheneuf, G.; Laurence, C. *Spectrochim. Acta* **1978**, *34A*, 15.
(37) Lide, D. R., Ed. *CRC Handbook of Chemistry and Physics*, 78th ed.; CRC Press: Boca Raton, FL, 1997.
(38) Møller, C.; Plesset, M. S. *Phys. Rev.* **1934**, *46*, 618.
(39) Head-Gordon, M.; Pople, J. A.; Frisch, M. J. *Chem. Phys. Lett.* **1988**, *153*, 503.
(40) Kohn, W.; Sham, L. J. *Phys. Rev.* **1965**, *A140*, 1113.
(41) Jho, J. Y.; Yee, A. F. *Macromolecules* **1991**, *24*, 1905.
(42) Xiao, C.; Yee, A. F. *Macromolecules* **1992**, *25*, 6800.
(43) Hörth, F. J.; Kuhn, K. J.; Mertes, J.; Hellmann, G. P. *Polymer* **1992**, *33*, 1223.
(44) Bailly, Ch.; Daumerie, M.; Legras, R.; Mercier, J. P. *J. Polym. Sci., Polym. Phys. Ed.* **1985**, *23*, 751.
(45) Krimm, S.; Abe, Y. *Proc. Natl. Acad. Sci. U.S.A.* **1972**, *69*, 2788.
(46) Snyder, R. G. *J. Chem. Phys.* **1967**, *47*, 1316.
(47) Strobl, G. R.; Hagedorn, W. *J. Polym. Sci., Polym. Phys. Ed.* **1978**, *16*, 1181.
(48) Mandelkern, L. *Acc. Chem. Res.* **1990**, *23*, 381.
(49) Mandelkern, L.; Alamo, R. G. *Macromolecules* **1995**, *28*, 2988.
(50) Guenet, J. M. *Thermoreversible Gelation of Polymers and Biopolymers*; Academic Press: New York, 1992.

MA9807623